Impact of Double DVCS in current and new experiments

Víctor Martínez-Fernández

PhD student at the National Centre for Nuclear Research (NCBJ, Warsaw, Poland)

NATIONAL CENTRE FOR NUCLEAR RESEARCH ŚWIERK

Work in collaboration with:

Katarzyna Deja (NCBJ)
Bernard Pire (CPHT)
Paweł Sznajder (NCBJ)
Jakub Wagner (NCBJ)

Work published in:
PRD 107 (2023), no. 9, 094035, hep-ph/2303.13668

Outline

- **Preliminaries:** DIS vs DVCS
- Double deeply virtual Compton scattering **(DDVCS)**
  - Why DDVCS?
  - Formulation *à la* Kleiss & Stirling (KS)
  - Tests of our KS-based formulation
  - Observables and MC simulations
- Summary and conclusions

Deep Inelastic Scattering (DIS)

- R. Hofstader & R. W. McAllister, Phys. Rev. **98**, 217 (1955) $\rightarrow$ elastic scattering $\rightarrow$ proton is an extended object of radius $\sim 10^{-13}$ cm
- M. Breidenbach et al., PRL **23**, 935 (1969) $\rightarrow$ DIS $\rightarrow$ proton is a composite object

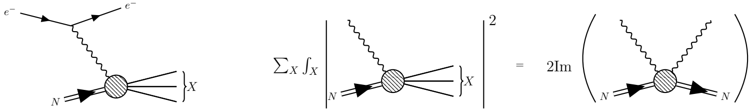

DIS (left), optical theorem (right - sum over X states = inclusiveness)

$$\sigma_{\gamma N\to X}=\sum_f \int_0^1 dx\;\sigma_{\gamma \mathfrak{q}_f\to X}(x)\mathrm{PDF}_f(x),\quad f=\text{flavor}$$

$$\mathrm{PDF}_f(x)=\frac{1}{2}\int \frac{dz^-}{2\pi}e^{ix\bar{p}^+z^-}\langle N|\bar{\mathfrak{q}}_f(-z/2)\gamma^+\mathcal{W}[-z/2,z/2]\mathfrak{q}_f(z/2)|N\rangle\Big|_{z_\perp=z^+=0}$$

Deeply Virtual Compton Scattering (DVCS)

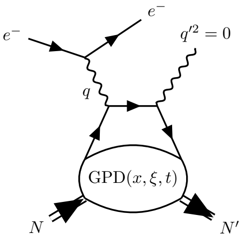

DVCS

- In the late '90s, Ji, Müller and Radyushkin introduced the Generalized Parton Distributions (GPDs) through DVCS process
- GPDs enter amplitude at LO via CFF:

$$\mathrm{CFF}_{\mathrm{DVCS}} \sim \mathrm{PV}\left(\int_{-1}^{1} dx \frac{1}{x-\xi} \mathrm{GPD}(x,\xi,t)\right) - \int_{-1}^{1} dx \;\, i\pi\delta(x-\xi)\mathrm{GPD}(x,\xi,t) + \cdots$$

Generalized Parton Distribution

GPD

Generalized Parton Distribution ≈ "3D version of a PDF (Parton Distribution Function)." With x the fraction of the hadron's longitudinal momentum carried by a quark:

$$\mathrm{GPD}_f(x,\xi,t) = \frac{1}{2}\int \frac{dz^-}{2\pi} e^{ix\bar{p}^+z^-} \langle N'(p')|\bar{\mathfrak{q}}_f\left(-\frac{z}{2}\right)\gamma^+\mathcal{W}[-z/2,z/2]\mathfrak{q}_f\left(\frac{z}{2}\right)|N(p)\rangle\Big|_{z_\perp=z^+=0}$$

$$t=\Delta^2=(p'-p)^2, \quad \xi=-\frac{\bar{q}\Delta}{2\bar{p}\bar{q}}, \quad \rho=\frac{-\bar{q}^2}{2\bar{p}\bar{q}}, \quad \bar{q}=\frac{q+q'}{2}, \quad \bar{p}=\frac{p+p'}{2}$$

Importance

- Connected to QCD energy-momentum tensor, and so to spin. GPDs are a way to address the hadron's **spin puzzle**
- **Tomography**: distribution of quarks in terms of the longitudinal momentum and in the transverse plane

$$q(x,\mathbf{b}_\perp)=\int \frac{d^2\mathbf{\Delta}}{4\pi^2}\ e^{-i\mathbf{b}_\perp\cdot\mathbf{\Delta}}H^q(x,0,t=-\mathbf{\Delta}^2) \leftrightarrow H^q\text{: a particular GPD}$$

Limitations of DVCS

- **Problem:** currently, GPDs are accessible experimentally in processes such as deeply virtual (DVCS) and timelike Compton scattering (TCS), but the LO amplitudes are restricted to the line $x = \pm\xi$

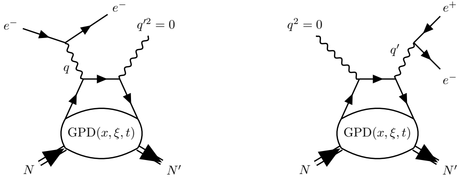

DVCS (left), TCS (right)

- GPDs enter amplitude at LO via CFF:

$$\mathrm{CFF}_{\mathrm{DVCS}} \sim \mathrm{PV}\left(\int_{-1}^{1} dx \frac{1}{x-\xi} \mathrm{GPD}(x,\xi,t)\right) - \int_{-1}^{1} dx \;\; i\pi\delta(x-\xi)\mathrm{GPD}(x,\xi,t) + \cdots$$

Similarly for TCS with $\xi \to -\xi$

Need to go beyond: Double DVCS (DDVCS)

- **Solution by DDVCS:** the extra virtuality allows for the introduction of a new (generalized) Björken variable ρ so that we can access GPDs for $x = \rho \neq \xi$

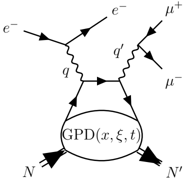

Double DVCS (DDVCS)

- GPDs enter amplitude at LO via CFF:

$$\mathrm{CFF}_{\mathrm{DDVCS}} \sim \mathrm{PV}\left(\int_{-1}^{1} dx \frac{1}{x-\rho} \mathrm{GPD}(x,\xi,t)\right) - \int_{-1}^{1} dx \;\; i\pi\delta(x-\rho)\mathrm{GPD}(x,\xi,t) + \cdots$$

$$\rho = -\frac{\bar{q}^2}{2\bar{p}\bar{q}}, \quad \xi = \frac{-\bar{q}\Delta}{2\bar{p}\bar{q}}$$

Original papers in DDVCS: Belitsky & Muller, PRL 90, 022001 (2003); Guidal & Vanderhaeghen, PRL 90, 012001 (2003); Belitsky & Muller, PRD 68, 116005 (2003)

Formulation *à la* Kleiss-Stirling

- In the view of new experiments, revisiting DDVCS is timely: **PRD 107 (2023), no. 9, 094035 (our work)**
- Rederivation of DDVCS' formulae via Kleiss-Stirling's methods:
  - **Amplitudes as complex-numbers**
  - 2 scalars as building blocks. For a and b as lightlike vectors:

$$s(a,b) = \bar{u}(a,+)u(b,-) = -s(b,a)$$

$$t(a,b) = \bar{u}(a,-)u(b,+) = [s(b,a)]^*$$

$$s(a,b) = (a^2 + ia^3)\sqrt{\frac{b^0 - b^1}{a^0 - a^1}} - (a \leftrightarrow b)$$

Kleiss & Stirling, Nuclear Physics B262 (1985) 235-262

DDVCS *à la* Kleiss-Stirling

- DDVCS amplitude:

$$i\mathcal{M}_{\rm DDVCS}=\frac{-ie^4}{(Q^2-i0)(Q'^2+i0)}\left(i\mathcal{M}^{(V)}_{\rm DDVCS}+i\mathcal{M}^{(A)}_{\rm DDVCS}\right)$$

- Vector contribution:

$$i\mathcal{M}^{(V)}_{\rm DDVCS}=-\frac{1}{2}\Big[f(s_\ell,\ell_-,\ell_+;s,k',k)-g(s_\ell,\ell_-,n^\star,\ell_+)g(s,k',n,k)-g(s_\ell,\ell_-,n,\ell_+)g(s,k',n^\star,k)\Big]$$
$$\times\Big[(\mathcal{H}+\mathcal{E})[Y_{s_2s_1}g(+,r'_{s_2},n,r_{s_1})+Z_{s_2s_1}g(-,r'_{-s_2},n,r_{-s_1})]-\frac{\mathcal{E}}{M}\mathcal{J}^{(2)}_{s_2s_1}\Big]$$

- Axial contribution:

$$i\mathcal{M}^{(A)}_{\rm DDVCS}=\frac{-i}{2}\epsilon^{\mu\nu}_{\perp}j_\mu(s_\ell,\ell_-,\ell_+)j_\nu(s,k',k)\Big[\widetilde{\mathcal{H}}\mathcal{J}^{(1,5)+}_{s_2s_1}+\widetilde{\mathcal{E}}\frac{\Delta^+}{2M}\mathcal{J}^{(2,5)+}_{s_2s_1}\Big]$$

DVCS & TCS limits of DDVCS

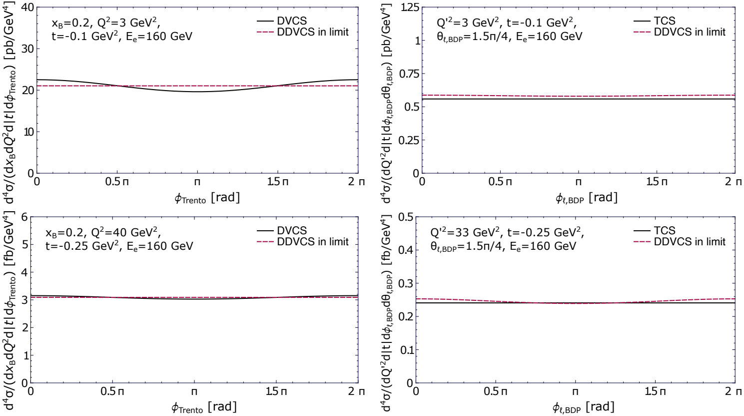

Comparison of DDVCS and (left) DVCS and (right) TCS cross-sections for pure VCS subprocess. **GK model for GPDs.**

Trento: PRD 70, 117504 (2004); **BPD:** EPJC23, 675 (2002)

Observables: cross-section

- For unpolarized beam and target:

$$\sigma_{UU}(\phi_{\ell,\mathrm{BDP}}) = \int_0^{2\pi} d\phi \int_{\pi/4}^{3\pi/4} d\theta_{\ell,\mathrm{BDP}} \ \sin\theta_{\ell,\mathrm{BDP}}$$

$$\times \left(\frac{d^7\sigma^{\rightarrow}}{dx_B dQ^2 dQ'^2 d|t| d\phi d\Omega_{\ell,\mathrm{BDP}}} + \frac{d^7\sigma^{\leftarrow}}{dx_B dQ^2 dQ'^2 d|t| d\phi d\Omega_{\ell,\mathrm{BDP}}} \right)$$

- Cosine components:

$$\sigma_{UU}^{\cos\left(n\phi_{\ell,\mathrm{BDP}}\right)}(\phi_{\ell,\mathrm{BDP}}) = M_{UU}^{\cos\left(n\phi_{\ell,\mathrm{BDP}}\right)} \cos\left(n\phi_{\ell,\mathrm{BDP}}\right)$$

- Cosine moments:

$$M_{UU}^{\cos\left(n\phi_{\ell,\mathrm{BDP}}\right)} = \frac{1}{N} \int_0^{2\pi} d\phi_{\ell,\mathrm{BDP}} \cos\left(n\phi_{\ell,\mathrm{BDP}}\right) \sigma_{UU}(\phi_{\ell,\mathrm{BDP}})$$

$N = 2\pi$ for $n = 0$, $N = \pi$ for $n > 0$.

Observables: cross-section

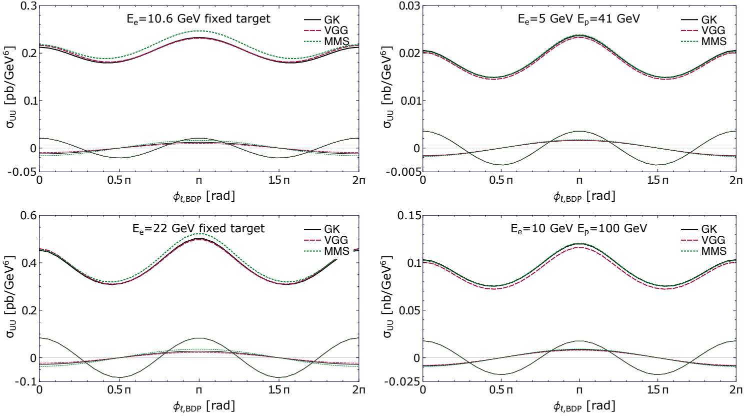

JLab12, JLab20+ | EIC 5x41, EIC 10x100

Experiment	Beam energies [GeV]	y	$\|t\|$ [GeV^2]	Q^2 [GeV^2]	Q'^2 [GeV^2]
JLab12	$E_e = 10.6,\ E_p = M$	0.5	0.2	0.6	2.5
JLab20+	$E_e = 22,\ E_p = M$	0.3	0.2	0.6	2.5
EIC	$E_e = 5,\ E_p = 41$	0.15	0.1	0.6	2.5
EIC	$E_e = 10,\ E_p = 100$	0.15	0.1	0.6	2.5

Observables: beam-spin asymmetry

- Single beam-spin asymmetry for longitudinally polarized electrons:

$$A_{LU}(\phi_{\ell,\mathrm{BDP}}) = \frac{\Delta\sigma_{LU}(\phi_{\ell,\mathrm{BDP}})}{\sigma_{UU}(\phi_{\ell,\mathrm{BDP}})}$$

$$\Delta\sigma_{LU}(\phi_{\ell,\mathrm{BDP}}) = \int_0^{2\pi} d\phi \int_{\pi/4}^{3\pi/4} d\theta_{\ell,\mathrm{BDP}} \ \sin\theta_{\ell,\mathrm{BDP}}$$

$$\times \left(\frac{d^7\sigma^{\rightarrow}}{dx_B dQ^2 dQ'^2 d|t| d\phi d\Omega_{\ell,\mathrm{BDP}}} - \frac{d^7\sigma^{\leftarrow}}{dx_B dQ^2 dQ'^2 d|t| d\phi d\Omega_{\ell,\mathrm{BDP}}} \right)$$

- We consider $Q'^2 > Q^2$: our DDVCS is "more" timelike than spacelike

Observables: beam-spin asymmetry

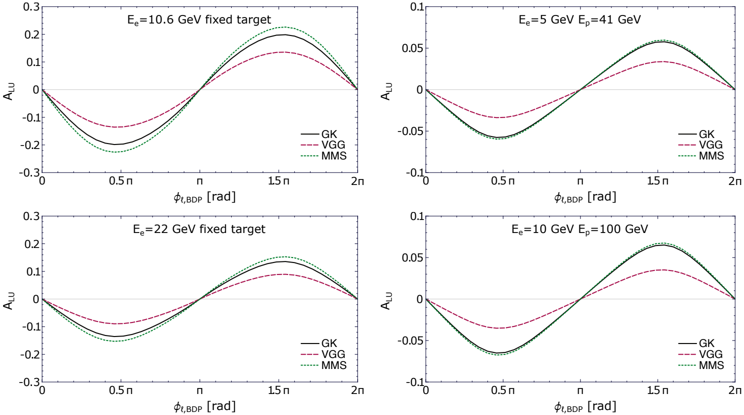

JLab12, JLab20+: up to **15-20%**

EIC 5x41, EIC 10x100: **3-7%**

Experiment	Beam energies [GeV]	y	$\|t\|$ [GeV^2]	Q^2 [GeV^2]	Q'^2 [GeV^2]
JLab12	$E_e = 10.6,\ E_p = M$	0.5	0.2	0.6	2.5
JLab20+	$E_e = 22,\ E_p = M$	0.3	0.2	0.6	2.5
EIC	$E_e = 5,\ E_p = 41$	0.15	0.1	0.6	2.5
EIC	$E_e = 10,\ E_p = 100$	0.15	0.1	0.6	2.5

Monte Carlo study: distribution in y

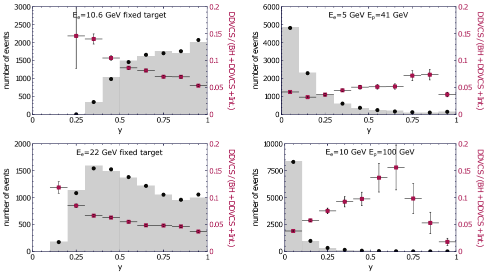

JLab12, JLab20+ EIC 5x41, EIC 10x100

EpIC MC
integrated cross-section
pure DDVCS fraction

Kinematic cuts:
$Q^2 \in (0.15, 5)$ GeV^2
$Q'^2 \in (2.25, 9)$ GeV^2
JLab: $-t \in (0.1, 0.8)$ GeV^2
EIC: $-t \in (0.01, 1)$ GeV^2
$\phi, \phi_\ell \in (0.1, 2\pi - 0.1)$ rad
$\theta_\ell \in (\pi/4, 3\pi/4)$ rad
JLab: $y \in (0.1, 1)$
EIC: $y \in (0.05, 1)$

10000 events/distribution. Neither acceptance nor detectors response are taken into account in this study

Experiment	Beam energies [GeV]	Range of $\|t\|$ [GeV^2]	$\sigma\|_{0<y<1}$ [pb]	$\mathcal{L}^{10k}\|_{0<y<1}$ [fb^{-1}]	$y_{\min}$	$\sigma\|_{y_{\min}<y<1}/\sigma\|_{0<y<1}$
JLab12	$E_e = 10.6,\ E_p = M$	$(0.1, 0.8)$	0.14	70	0.1	1
JLab20+	$E_e = 22,\ E_p = M$	$(0.1, 0.8)$	0.46	22	0.1	1
EIC	$E_e = 5,\ E_p = 41$	$(0.05, 1)$	3.9	2.6	0.05	0.73
EIC	$E_e = 10,\ E_p = 100$	$(0.05, 1)$	4.7	2.1	0.05	0.32

Summary and conclusions

- New analytical formulae for the electroproduction of a lepton pair have been derived.
- It is already implemented in PARTONS and EpIC MC (LO + LT).
- Asymmetries are large enough for DDVCS to be measurable at both current (JLab12) and future (JLab20+, EIC) experiments.
- Addressing GPD model dependence with cross-sections and asymmetries is possible.

Thank you!

Complementary slides

Models for the C-even part of GPD H

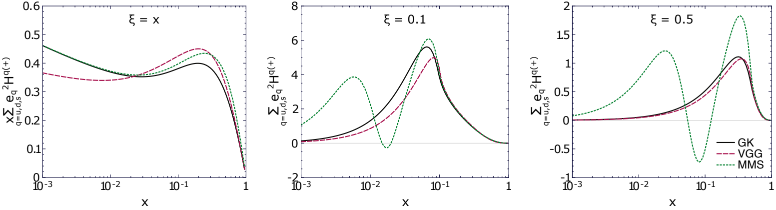

Distributions of $\sum_q e_q^2 H^{q(+)}(x, \xi, t)$ at $t = -0.1\ \mathrm{GeV}^2$, where $q = u, d, s$ flavours for (left) $\xi = x$, (middle) $\xi = 0.1$ and (right) $\xi = 0.5$. The solid black, dashed red and dotted green curves describe the GK, VGG and MMS GPD models, respectively. The C-even part of a given vector GPD is defined as:
$H^{q(+)}(x, \xi, t) = H^q(x, \xi, t) - H^q(-x, \xi, t)$. The scale is chosen as $\mu_F^2 = 4\ \mathrm{GeV}^2$.